# EXPLORING THE LIMITS OF OCCUPANT SAFETY IN FRONTAL CAR-HGV IMPACTS

**Shweta Joshi, Robert Thomson, Jim Brouzoulis**
Chalmers University of Technology, Sweden
**Rikard Fredriksson**
Swedish Transport Administration, Sweden; Chalmers University of Technology, Sweden
**Krystoffer Mroz**
Autoliv Research, Sweden
**Fredrik Törnvall**
Volvo Group AB, Sweden
**Reimert Sjöblom**
Scania AB, Sweden

## ABSTRACT

Car occupant fatalities are overrepresented in car-Heavy Goods Vehicle (HGV) frontal impacts even with legislated crashworthiness requirements for both vehicle types. While most modern passenger cars in Europe exceed mandated safety levels by a wide margin, protecting occupants in car-HGV frontal impacts remains a major challenge. An offset frontal crash test (Test-1) conducted in Sweden highlighted that the front structures currently used in HGVs cannot fully engage with the front structures of a 5-star Euro NCAP-rated passenger car and absorb only a limited share of the crash energy. A new study and follow-up test (Test-2) were conducted to explore potential improvements in HGV design. In Test-1, the HGV's Front Underrun Protection (FUP) beam fractured early in the impact, resulting in minimal energy absorption by the frontal structures. The car experienced extensive deformation because its longitudinal crash beams were not effectively engaged. Two key areas of improvement were identified: (1) horizontal load distribution across HGV FUP system and (2) energy absorption potential. A simulation study using a simplified HGV model was performed to develop an experimental front structure with integrated FUP to improve crash performance, taking advantage of the EU's new regulation for extended HGV fronts. Improved load distribution was achieved by using a steel backup plate supported by bracing integrated into existing truck structures. A honeycomb structure based on the IIHS 2.0 side impact barrier was developed to improve energy absorption. The barrier's geometry was designed to align with known passenger car interaction zones, thereby promoting activation of energy-absorbing components. The follow-up test (Test-2) was conducted with the experimental HGV front and compared with Test-1. The passenger car benefited from horizontal load distribution in Test-2 which reduced the deformation around the A-pillar and door. However, higher intrusions were observed in the driver's seating area. The maximum acceleration recorded in the baseline test was 75g, which was reduced to 58g in the second test, closer to Euro NCAP MPDB test results (35g) for the same car. The impact energy in both tests was significantly higher than in any previous car-HGV impact study. The results demonstrated that dynamic loading of the HGV front imposes structural demands different from those assessed by the quasi-static UN R93 test requirements. The severity levels in this study reflect conditions possible in real-world traffic (even in low-speed urban environments), but they exceed practical thresholds for current design and regulatory frameworks. Future regulatory and consumer testing that integrate 1) active safety systems that reduce collision speed and mitigate crash severity with 2) improved structural performance will promote vehicle designs that address common crash scenarios on rural and urban roads.

## INTRODUCTION

Heavy Goods Vehicles (HGVs) are essential to transport goods and services worldwide, complementing railways and marine transport. In Sweden, HGVs weighing over 3.5 tonnes make up only 5% of total vehicle mileage, while cars account for 81% [1]. Despite this, HGVs are involved in 23% (2022) of all road traffic fatalities [2, 3]. In accidents involving HGVs and cars, the significant mass difference often results in fatal outcomes for car occupants and is a concern worldwide.

In Europe, road accidents injured more than 1.14 million people and resulted in approximately 20,400 fatalities in 2023. The latest research from the Community database on Crashes on the Roads in Europe (CARE) indicates that the highest number of fatal crashes involved car occupants (44%), followed by pedestrians (18%), motorcyclists (17%), Cyclists (10%), Light Goods Vehicles (3%), Mopeds (2%) and HGV occupants over 3.5 tonnes only accounted for 2% of fatalities [4]. An IIHS analysis based on the US Department of Transportation's Fatality Analysis Reporting System (FARS) raised concerns about the fatalities due to the higher structural and mass differences between HGVs with GVWR (Gross Vehicle Weight Rating) greater than 10,000 pounds compared to other vehicles on the road [5]. In 2023, 11% (4,354) of all 40,901-road traffic fatalities in the U.S. involved crashes with HGVs including tractor-trailers and single-unit HGVs. Among these HGV-related fatalities, 65% were occupants of passenger cars, 16% were occupants of HGVs, and 17% were other road users. Of the occupants killed in two-vehicle crashes involving a passenger vehicle and an HGV, 97% were the occupants of the passenger vehicles [5]. The high fatality rate for passenger cars colliding with HGVs has led to considerable research on improving road infrastructure and vehicle safety systems. In 2020, the SAFE-UP project [6] was launched in Europe to make future mobility safer for all road participants. The researchers studied 2085 car-car and car-HGV accidents in different traffic scenarios from the German In-Depth Accident Study (GIDAS) database. They revealed that head-on car-to-HGV (>3.5tonne) accidents are the most common type of fatal accidents involving these two vehicle types, mostly occurring on rural roads [7].

To develop an understanding of crash severity in a fatal scenario, an exploratory car-to-HGV frontal crash test was conducted in Sweden. A Euro NCAP 5-star rated passenger car collided head-on with a latest-generation HGV equipped with a Front Underrun Protection Device (FUPD). Both vehicles were travelling at 50 km/h, with a 50% frontal overlap for the car. The fatal crash analysis supporting this baseline test, Test-1 [8], showed that more than 50% of frontal crashes between cars and HGVs on Swedish roads occur at speed limits of 70–80 km/h, which can result in closing speeds up to 160 km/h (pre-crash braking is unknown). This is consistent with findings from the European mobility project SAFE-UP, which reported a median closing speed of approximately 75 km/h [6]. The energy in this crash test was substantial and could be reached in real crash scenarios. The results showed severe damage to the passenger car, severe occupant injuries, and damage to the HGV's front structure and steering mechanism. Test-1 demonstrated that current HGV designs do not adequately protect car occupants in frontal collisions, especially when the impact involves 50% or less of the HGV's width. This underscored the need for improved energy management in crashes involving cars and HGVs. Additionally, it raised concerns about the HGV's maneuverability after a collision.

### Current Safety Standards for HGVs

Car manufacturers have been developing new safety systems and institutions like Euro NCAP, IIHS, and NHTSA have been introducing testing protocols and consumer ratings to objectively assess vehicle safety. Driven by research, innovation, stricter regulations, and increasingly influential commercial rating programs, the automotive industry has strengthened protection for both vulnerable road users and car occupants. In Europe, more than 83% of cars achieve a 4–5-star Euro NCAP rating [9]. However, gaps remain in protecting car occupants in accidents involving HGVs, which can weigh 10 to 30 times more than cars. Legislative measures such as UN R93 [10] have been established to address the issue of car underrun in frontal collisions with the HGV. Still, they are insufficient to accurately represent the dynamic loading of an actual frontal collision involving a HGV and a car [11]. FUP systems in HGVs only have to demonstrate compliance with legislative requirements and there is no comparable consumer assessment program to enhance truck crashworthiness beyond the legislated minimum.

The VC-COMPAT project (2007) evaluated FUP systems in HGVs using crash tests where a car collided with a stationary HGV at 75% overlap and up to 75 km/h speeds [12]. These experimental conditions did not reflect real-world collisions, where both vehicles are in motion and the overlap is often less than 50% of the truck’s width. In real-life crashes, the HGV experiences only a small change in velocity and continues to move forward, while the passenger car is subjected to much higher deceleration and nearly double the change in velocity compared with the VC-COMPAT test conditions. The large momentum difference between the two vehicles plays a major role in crash dynamics, which was not captured under the VC-COMPAT test setup. As a result, the injury values and deformation levels recorded in the test were less severe than those seen in more recent crash studies [8]. Even with these limitations, VC-COMPAT results provide valuable insights. In offset crashes (72–75% car overlap) at 75 km/h, energy-absorbing FUP systems reduced ASI (Acceleration Severity Index) values by about 9% compared to rigid FUPs and lowered passenger car deformation, as the FUP absorbed around 16% of the total impact energy [12]. Until recently, HGVs have limited deformation zones for energy absorption capacity due to dimensional restrictions, Regulation (EU) 2019/1242 now allows for longer HGV geometries. This creates an opportunity to increase energy absorption potential and improve crash outcomes in future HGV designs.

### Research Objectives

This study builds on the principles to improve occupant protection identified in a previous car-to-HGV frontal impact test [8] An experimental HGV front end structure was to be developed to promote lateral load spreading and energy absorption by the HGV beyond those observed in previous research. The new HGV front was tested under the same conditions as the baseline test in [8].

The goal is to observe how the experimental HGV front-end performs in comparison to a production vehicle and identify the scope for safety improvements. Criteria used to evaluate compatibility performance include analysis of:(1) the accelerations and deformations of the passenger car (2) deformation to sensitive areas of the HGV such as the steering and braking systems.

## METHODOLOGY

### Development of Experimental HGV Front

A Finite Element (FE) study with LS-Dyna was used to define the experimental HGV front structures for Test-2. A FE model of a generic European cab-over-engine HGV developed by the European Commission's Joint Research Centre (JRC) for vehicle security barrier testing was used for the HGV [13]. The front of this HGV model was modified and adapted for FE analysis with new front structures. For the passenger car, the study used a FE model of the mid-size sedan, NHTSA 5-star and IIHS "Good/Top Safety Pick+" rated Honda Accord (Model Year 2014), which is different from the Seat Leon 2021 car used in actual testing (Figure 1). There are differences in the car bumper beam and subframes; thus, only the global behavior of the car and its interaction with the experimental front was analysed in the FE study.

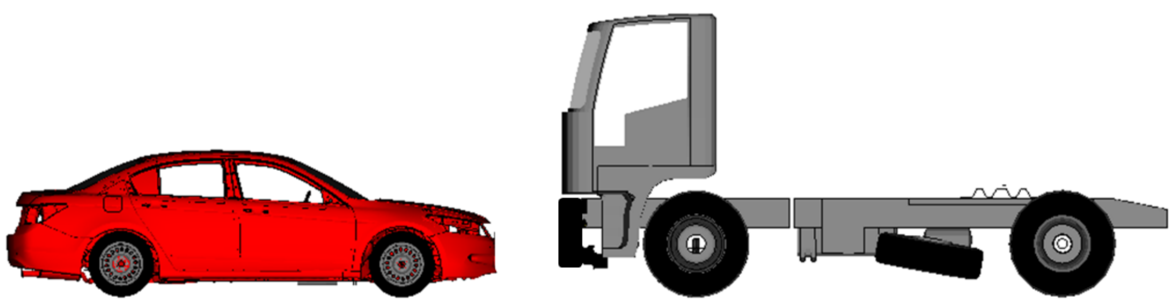

***Figure 1: FE model for - Passenger car (1.57 tonnes) and HGV (28 tonnes).***

The experimental HGV front was based on the IIHS 2.0 side impact deformable barrier. The IIHS 2.0 barrier has several honeycomb elements with different crush strengths shown by different shading in Figure 2 b). A softer (140 kPa) upper element sits on top of the stiffer (1100 kPa) rail elements and middle element (325 kPa). Bumpers are represented with 325 kPa honeycomb elements mounted on the forward cladding of the main barrier block. The objective of this barrier is to duplicate the stiff longitudinal members of pickup trucks as they load the softer structures of a car during a side impact. Technical specifications of the barrier are available from IIHS[14].

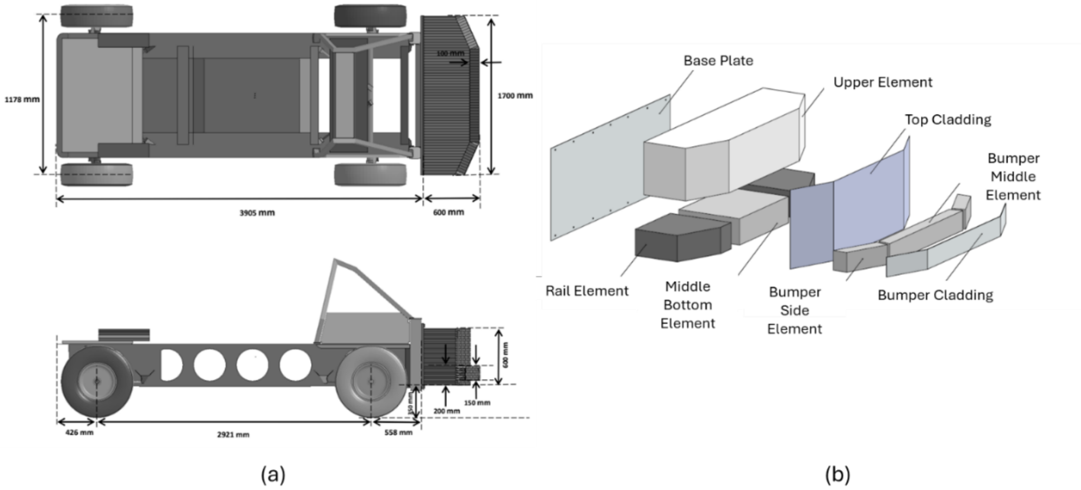


***Figure 2: IIHS 2.0 side impact deformable barrier- (a) Barrier mounted on trolley (b) Exploded View [14].***

Observations from Test-1 were used to develop the experimental HGV front for Test-2. In Test-1, the FUP section was positioned lower than the car's structural members, as shown in Figure 3. The FIMCAR full-width impact testing shows that the region between 330 and 580 mm is critical for promoting structural interaction [15]. Crash compatibility can be improved by aligning the geometry of load-bearing structures and integrating energy-absorbing components along the load path. The following considerations were applied in the design of the honeycomb HGV front:

- FUP failure is undesirable and may lead to instability in the interaction with the oncoming passenger car. An optimal balance between strength and energy absorption must be achieved. The honeycomb section was divided into three upper and four lower sections where a Finite Element (FE) study was used to establish the stiffness values of these sections (Figure 7).
- The kinetic energy involved in both Test-1 and Test-2 was approximately 3000 kJ. In such a severe collision, it is not feasible for the car or HGV's crash structures to completely absorb the energy. Instead of relying on prolonged engagement between the vehicles, the HGV front geometry was designed such that the passenger car slides past the HGV with limited rearward rebound.
- Barrier manufacturing constraints, like cell size, foil thickness, assembly tooling, etc. constrained the final geometry and stiffness range of the barrier.


***Figure 3: Test-1, Vertical alignment of main frontal structures.***

**Crash Test Setup**

A crash test between the HGV with experimental front and a passenger car was conducted with 50% overlap of the car width and a closing speed of 100 km/h identical to Test-1 (Figure 4). The passenger car was a 2021 Seat Leon, rated 5 stars in Euro NCAP testing (conducted in 2020 under the latest protocol) for both tests. Total test weight of the passenger car was 1.57 tonnes, while the HGV had a test weight of 28 tonnes.

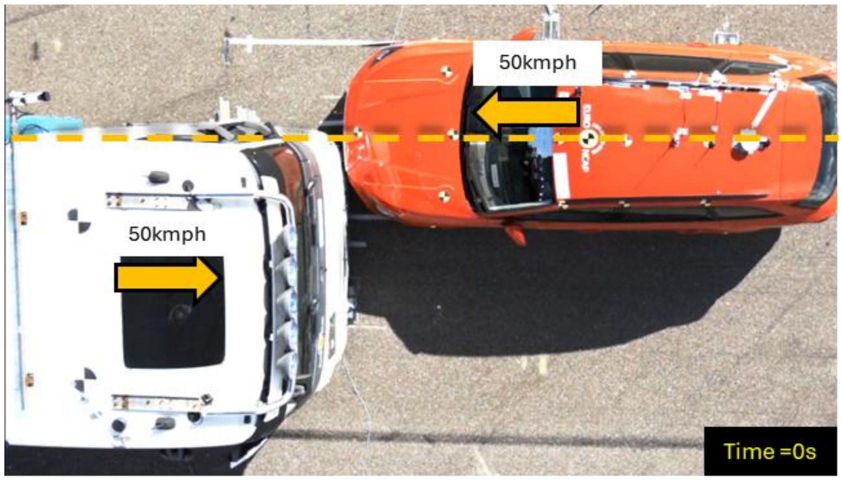


***Figure 4: 50% offset frontal impact between passenger car and HGV at 100 km/h closing speed.***

**Crash Evaluation Criteria**

The crash compatibility between the car and HGV with experimental front was evaluated using three measurement metrics: the occupant compartment's structural intrusion, vehicle acceleration pulse, and injury risk assessment for Hybrid III 50$^{th}$ percentile dummy. For the car, the X-acceleration pulse was measured on the left side near the B-pillar, and the change in velocity was analyzed from the same accelerometer [16]. It is crucial to evaluate structural intrusions in the car to measure the survival space for occupants. This study examined X-deformations in the A-pillar, door opening, interior footrest, toe pan, accelerator pedal, and steering column. Injury risk is assessed based on the Euro NCAP MPDB criteria, which evaluates potential injury risks across multiple body regions, with defined minimum and maximum thresholds [16].

## RESULTS

**Experimental HGV Front Design- Test-2**

FE simulations were performed to derive honeycomb stiffness and study the car's deformation and acceleration. The goal of improving lateral load spreading and energy absorption was achieved with an experimental FUP consisting of a backup plate mounted onto the chassis using brackets (Figure 5) and a honeycomb structure (Figure 6 & Figure 7). The backup plate was designed to protect critical components such as the steering gear, the linkage to the front axle and distribute crash loads and was angled outward beyond the frame rails to promote glance-off behavior during impact. The design and stiffness of the backup plate plays a critical role in improving self-protection, geometrical compatibility, and glance-off performance. Details on barrier characteristics are shown in Figure 7; these values were derived through the parametrical variation of the honeycomb stiffness with the goal of balancing the car B-pillar accelerations and door deformations observed in FE simulations. The bumper and lower middle honeycomb had the stiffest crush stiffness with lower stiffnesses in the upper and outer honeycomb elements.

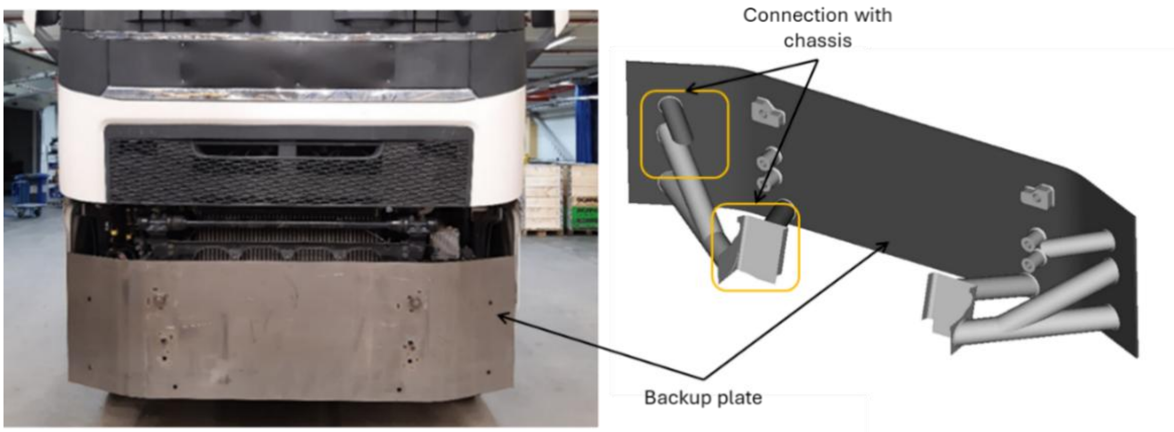


***Figure 5: Left side- HGV with backup plate, Right side- Initial CAD for backup plate with connection points to the chassis on Left and Right side (the actual backup geometry differed from the CAD).***

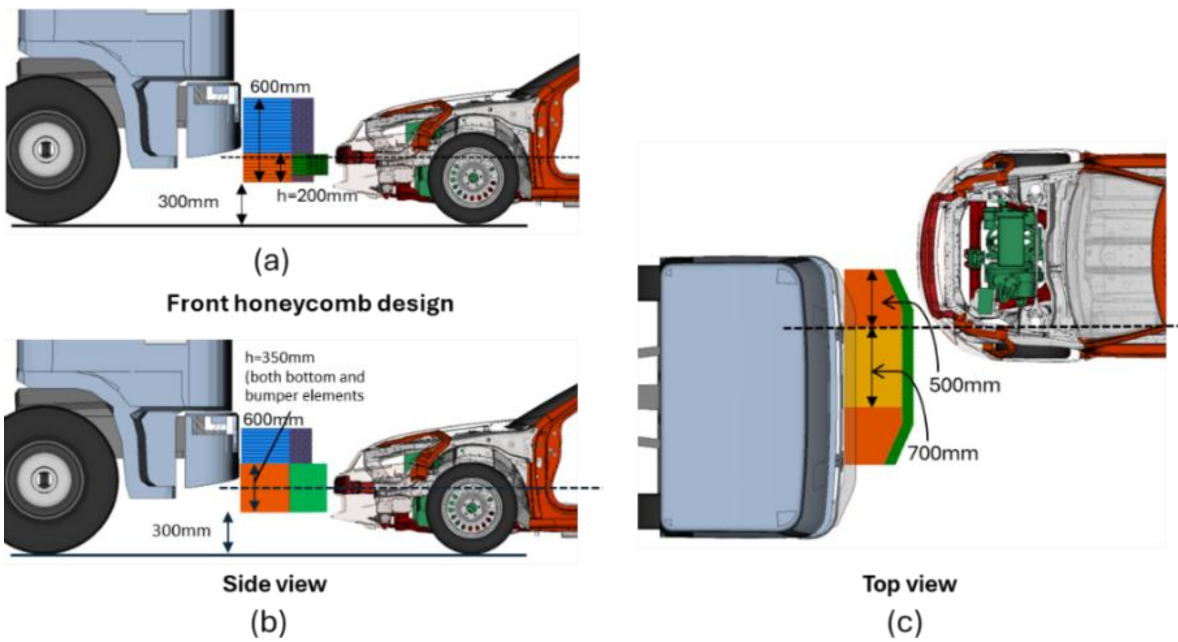


***Figure 6: Test-2, (a) Side view of IIHS 2.0 and (b) experimental HGV front with modifications, (c) image illustrates the lateral alignment of the two vehicles (Note: The car and HGV shown in the image are for illustration and not the tested vehicles).***

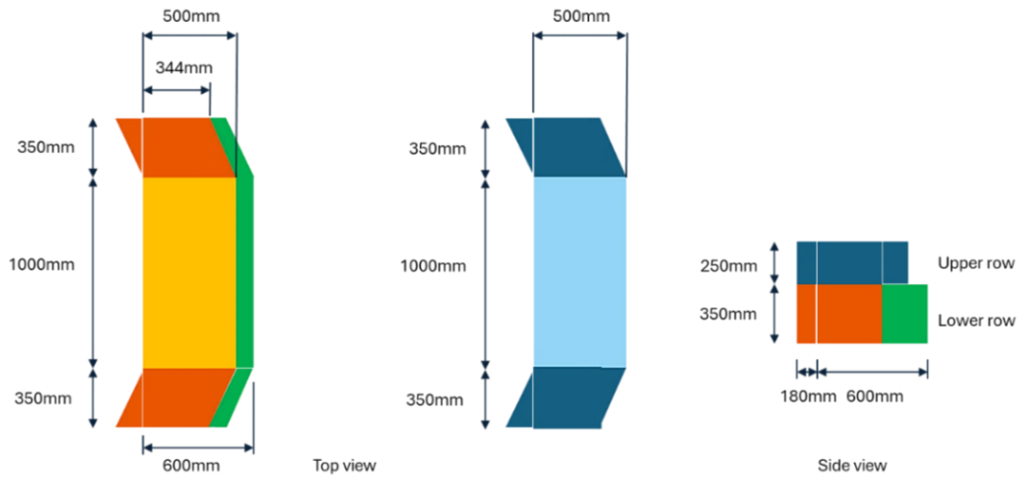


| Bottom row elements (parts) | Stiffness (MPa) | Upper row elements (parts) | Stiffness (MPa) |
|---|---|---|---|
| Bottom Rails (2) | 0.325 | Upper Rails (2) | 0.325 |
| Bottom Middle | 1.1 | Upper Middle | 1.1 |
| Bumper Sides (2) and Middle | 1.1 | Bottom wedges (2) | 0.325 |
| Bottom wedges (2) | 0.325 | | |

***Figure 7: Upper and Lower sections of Experimental HGV front with custom stiffness based on balance between acceleration pulse and deformation at critical locations on the car.***

FE simulation indicated that the car glances off to the side without further engagement with the experimental HGV front (Figure 8). FE analysis of the truck with experimental front exhibited three impact stages: Stage 1 corresponds to the initial contact with purely longitudinal car motion 0-65 ms, Stage 2 starts at 66 ms and is the start of lateral car motions until Stage 3 where loss of contact between the car and the HGV is observed.

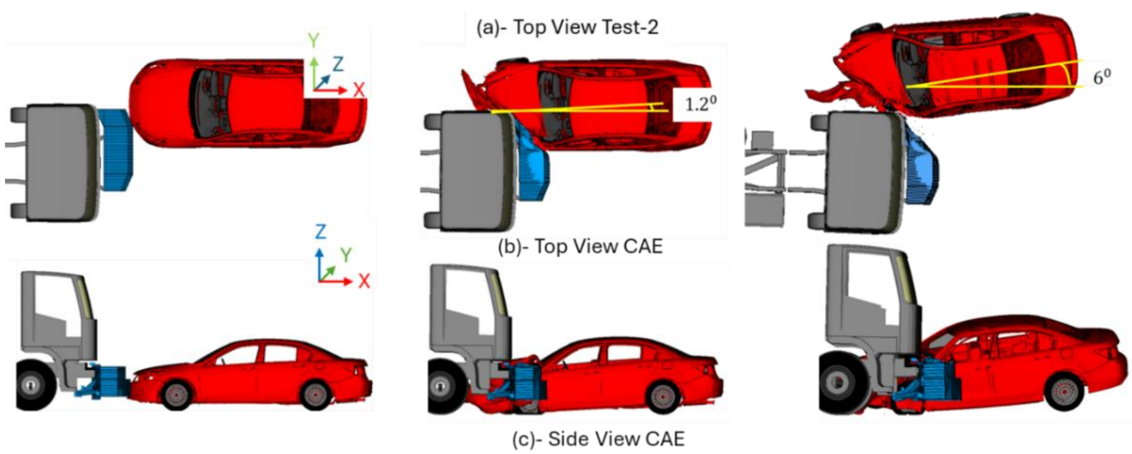


**Figure 8: FE simulation (top view) and (top and side view) at 0 ms, 66 ms and 160 ms in the 50% offset car to HGV frontal impact**

**Crash Test Results**

In both Test 1 and Test 2, the crash involved 3,000 kJ of energy, which tested the frontal crash protection limits of the vehicles. For the HGV, the damage was primarily to the front structures, affecting the truck's steering ability after the crash. The passenger car's occupant compartment was compromised, as shown in Figure 9. Structural intrusions were observed at points where occupants could contact with the interior (Figure 10).


***Figure 9: Deformed HGV and car structure in (a) Test-1 and (b) Test-2 after the frontal collision 50% offset impact between passenger car and HGV.***

In Test-1, the HGV FUP fractured (Figure 9 (a)) and exposed the cab's bottom to the car's structural members, causing damage to the HGV's steering system and puncturing its left front tire. This led to the HGV moving laterally after the impact. The car rotated after contacting the HGV in Test-1 and came to rest 30m from the impact point. The car's crush zone and longitudinal members remained relatively undamaged in the first test (Figure 9 (a)). In Test-2, with the experimental truck front, deformation of the door and A-pillar of the car showed significant improvements compared to Test-1 (Figure 9 (b)). Specifically, the change in door opening decreased by 64%, the deformation at the bottom of the A-pillar was reduced by 66%, and the top deformation of the A-pillar decreased by 35% (Figure 11). The intrusion values at the accelerator pedal, footrest, and toe-pan increased in Test-2 compared to Test-1. This difference in intrusion values can be attributed to the distributed horizontal and vertical loading in Test-2 due to the backup structure. The overall deformation of the car in Test-2 is shown in Figure 12.

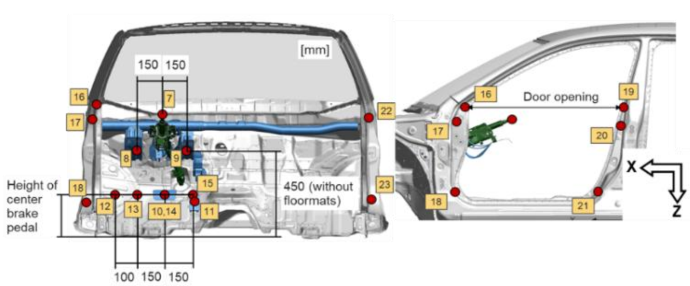


| Marker point location | Change (mm) | | |
|---|---|---|---|
| | X | Y | Z |
| Steering column DAB (7) | -77 | -169 | -8 |
| Interior IP (right knee) (9) | -44 | -352 | 19 |
| Accelerator pedal (11) | -35 | 52 | -54 |
| Brake pedal (10) | 10 | 38 | -21 |
| Brake pedal - Unloaded robot (14) | 0 | -12 | 5 |
| Interior Toepan (13) | -101 | -27 | 62 |
| Interior Left footrest (12) | -97 | -51 | 26 |
| A-pillar left Top (16) | -255 | 156 | -39 |
| A-pillar left Bottom (17) | -109 | 1 | 2 |
| B-pillar left Top (19) | 1 | -5 | -13 |
| B-pillar left Bottom (21) | -6 | 0 | -15 |
| A-pillar right Top (22) | -1 | -17 | 5 |
| A-pillar right Bottom (23) | 0 | -2 | 5 |
| Door Opening change | -256 | 162 | -26 |

***Figure 10: Structural intrusion of the tested car with image of intrusion measurement marker location, the table shows the X intrusion values with negative sign.***

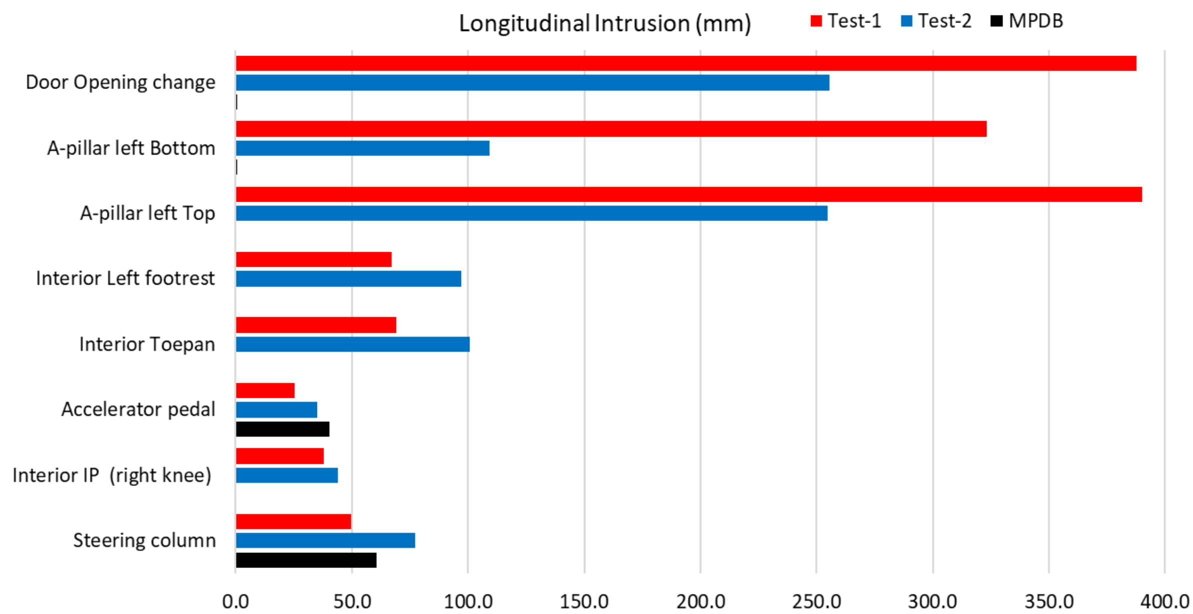


***Figure 11: Longitudinal intrusion at critical locations in the car for Test-1, Test-2 and EURO NCAP MPDB (2020) test.***

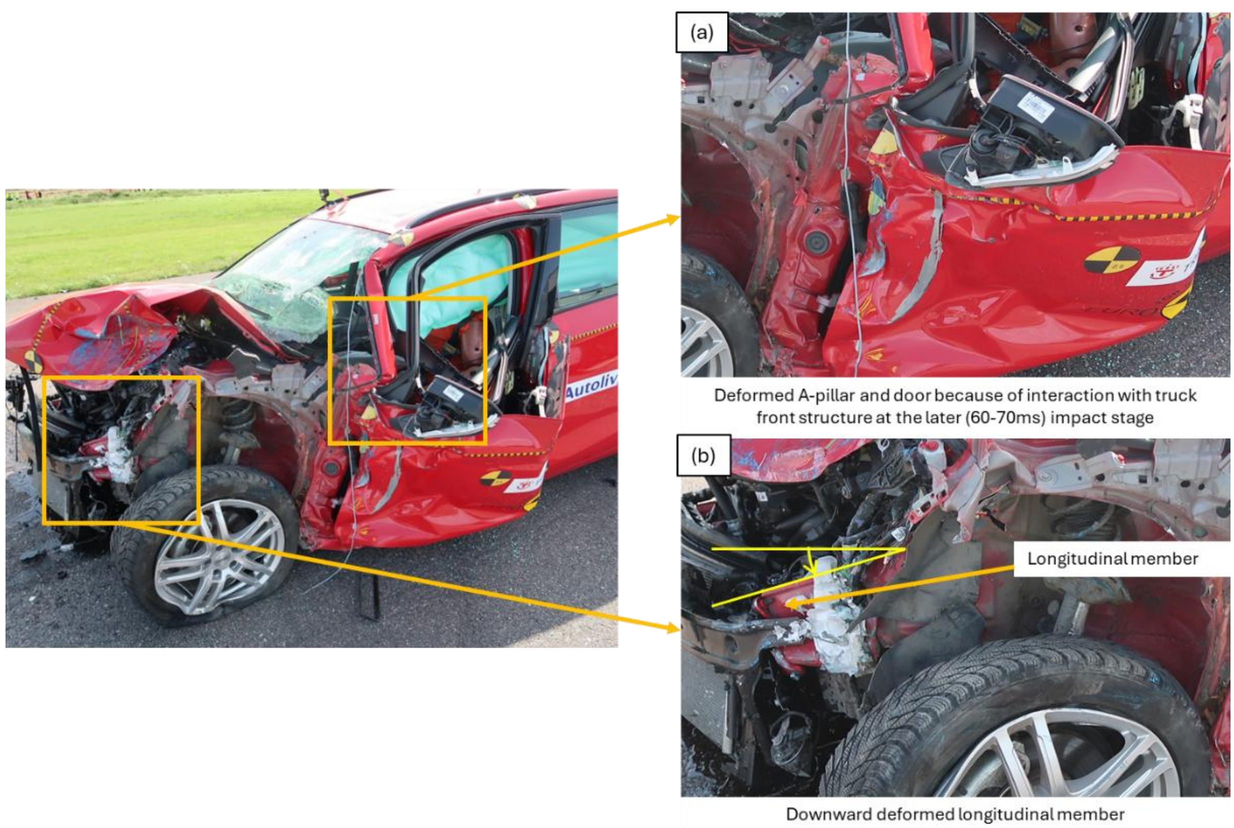


***Figure 12: Deformed car structures after Test 2.***

**Acceleration Assessment- Passenger Car**

In Test-2, the passenger car crash consists of four main events corresponding to the acceleration peaks (Figure 13**).** The initial impact peak of 22 g (t=5 ms) occurs when the sheet metal parts of the car's hood impacted with the protruded lower and stiffer section of the honeycomb structure. Around 30 ms after impact, the left wheel of the car starts loading the HGV front and eventually stops, while the right wheel continues to move forward until about 60ms. This asymmetric loading causes the front axle to detach during the later stages of the crash. A peak acceleration is observed at 57 ms during a local interaction between the longitudinal member of the car and the HGV front and backup plate. The car’s A-pillar was seen to contact the HGV's front at approximately 70 ms, when the car stops moving forward and is pushed downwards. During this sequence of events, the bumper's sheet metal parts get stuck to the deformed honeycomb in the front of the HGV. The simulation study had initially predicted that the car would glance off to the side. However, the passenger car structures continued to absorb impact energy while rotating 23° during the test.

Figure 13 shows these events in comparison to crash events in Test-1 at t = 36 ms, 57 ms and 200 ms respectively. In Test-1, the maximum acceleration reached by car occurred during the initial impact phase (36 ms) due to the immediate failure of the FUP system, which absorbed little to no energy. This caused the car to underrun truck chassis parts below the cab loading the car’s wheel, firewall, and A-pillar. Consequently, the car structure experienced greater deformation and an acceleration peak of 73g. The experimental FUP configuration demonstrated a gradual deceleration pulse with a significantly lower peak acceleration of 58g (at 57 ms), as shown in Figure 14. The vertical line in the graph represents the time at which the B-pillar acceleration peaked in Test-1. In Test-2, the experimental FUP delayed this peak and produced a more desirable energy absorption profile similar to the Euro NCAP car to MPDB test. The results from Test-2 highlight the potential benefits of designing an energy-absorbing, more compatible HGV front structure.

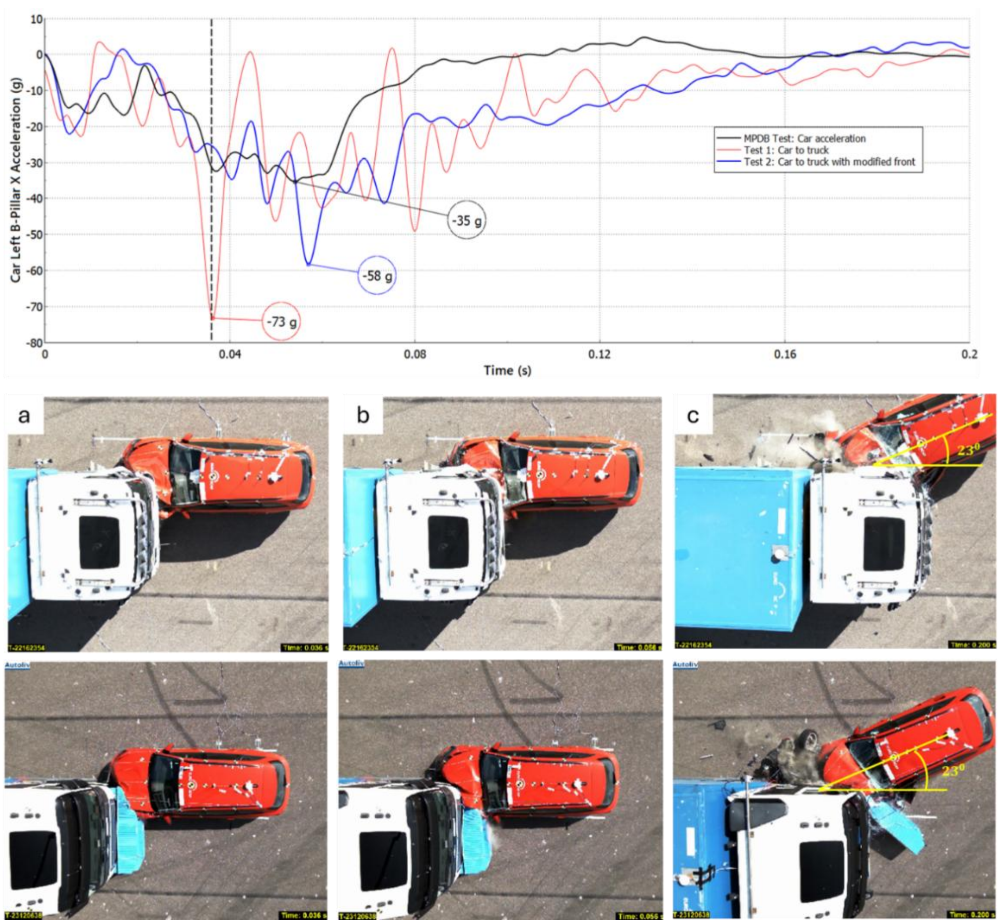


***Figure 13: Sequence of deformation during 50% offset frontal impact between passenger car and HGV in Test-1 and Test-2 at (a) 36 ms (Max acc peak Test-1), (b) 57 ms (Max acc peak Test-2), (c) 200 ms.***

During first 20 ms of impact, the car in Test-2 did not engage effectively with the experimental truck front compared to the MPDB test. Figure 13 shows how the magnitude of car acceleration increases in the first 10 ms but then drops suddenly to zero for both vehicle-vehicle tests. This is not apparent in the MPDB test where a consistent crush resistance of the barrier is seen in the crash pulse. Peak car accelerations in Test-2, from 30 to 50 ms, are comparable to those observed in the MPDB test and indicate renewed honeycomb crush resistance in the experimental truck front. The peak acceleration for both Test-2 and the MPDB occurred at the same time, 58g and 35g, respectively (Figure 13). This variation in the peak values was primarily due to: (1) the honeycomb structure in the HGV front bottoming-out locally at the contact point with the car's longitudinal member and, (2) the honeycomb HGV front was stiffer compared to MPDB barrier in Test-2 (Figure 14). It is important to note that the impact energy in Test-2 was significantly higher than that of the MPDB test.


***Figure 14: Deformation comparison for the car in the 50% offset frontal impact between (a) Test-2 (Passenger car and HGV), (b) car to MPDB in EURO NCAP test.***

**Occupant Kinematics and Injury Analysis**

Occupant kinematics and the car's motion at 55 ms, 75 ms, 100 ms, and 150 ms for Test-2 are shown sequentially in Figure 15. In Figure 15 (a), the dummy is restrained solely by the seatbelt for the first 60 ms during the impact. A peak chest acceleration of 81 g is recorded at 92 ms (Appendix A, Figure A1), which occurs between the states shown in Figure 15 (b) and (c). At around 70 ms, the dummy's head makes initial contact with the airbag but slips through the gap between the steering wheel and the A-pillar. Following this, the head continues moving in the Y-direction due to the vehicle motion to the right and deformation of the front axle. By 100 ms, the head becomes trapped between the dashboard and the deformed A-pillar. These interactions lead to elevated chest and head loading, resulting in high injury values.

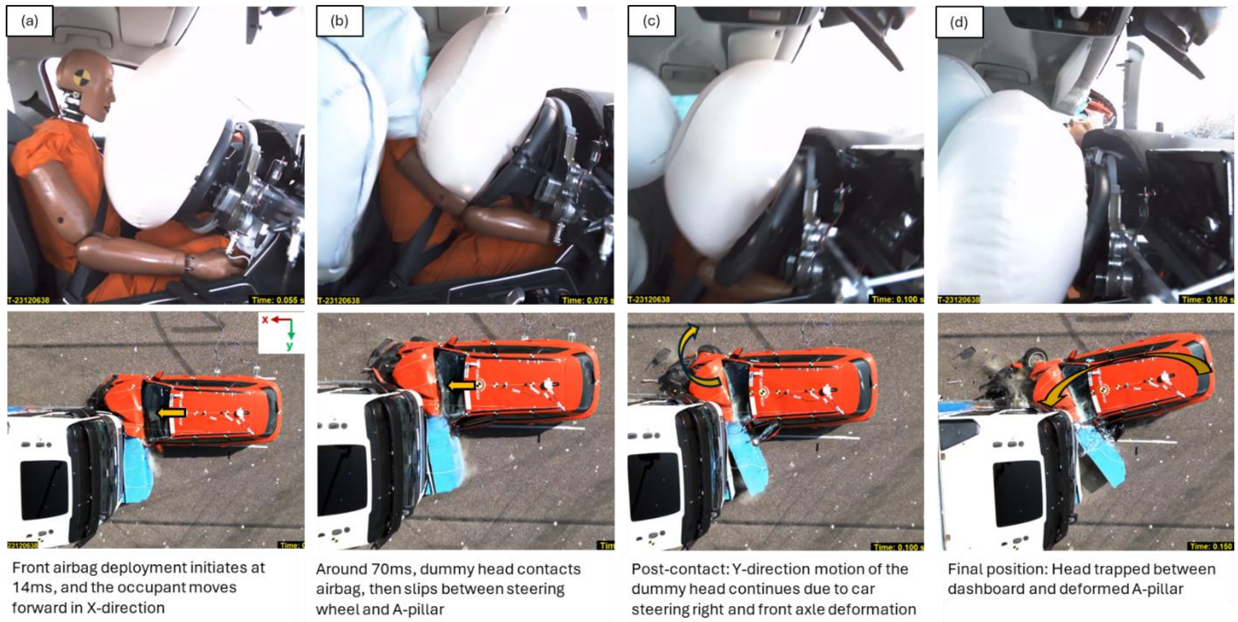


***Figure 15: Occupant kinematics and vehicle motion at 55ms, 75ms, 100ms, and 150ms during Left side 50% overlap frontal impact with HGV.***

Injury metrics recorded for the Hybrid III 50$^{th}$ percentile male dummy, as presented in Table 1**,** indicate severe forces exerted on the occupant, resulting in poor ratings for the head, chest, and lower body regions for Test-1 and Test-2. In Test-2, the Head Injury Criteria (HIC) values are rated as poor, primarily due to suboptimal interaction between the dummy's head and the front and side-curtain airbags. This is attributed to undesirable steering wheel kinematics and significant A-pillar deformation (Figure 15 (c and d). The extensive structural deformation caused the frontal airbag to displace laterally (towards the right) relative to the dummy's head trajectory, while the curtain airbag failed to provide lateral head support. The car's compromised structural integrity exposed the dummy to the A-pillar and dashboard surfaces. In combination with the vehicle's pitching and yawing motion, the dummy's head became entrapped between the deformed A-pillar and dashboard. This entrapment, along with contact with hard surfaces, contributed to elevated head injury values.

***Table 1: HIII 50$^{th}$ percentile male dummy injury results and rating for Test-1 and Test-2, derived according to the Euro NCAP 2020 frontal test protocol - Green=Good, Yellow=Adequate, Orange=Marginal, Brown=Weak, Red=Poor).***

| Injury parameters | Test-1 | Test-2 | Higher Performance Limit | Lower Performance Limit |
|---|---|---|---|---|
| Peak head resultant acc. (g) | 94.5 | 94.1 | 70 | 80 |
| HIC 15 | 754.4 | 754.6 | 500 | 700 |
| 3ms Head Clip (g) | 90.4 | 80 | 72 | 80 |
| Upper Neck Extension (Nm) | 38.9 | 28.4 | 42 | 57 |
| Thorax Compression Criteria (linear mm) | 32.6 | 37.5 | 22 | 42 |
| Thorax V*C (m/s) | 0.37 | 0.3 | 0.5 | 1 |
| Left Femur Force Criterion (N) | 7070.4 | 5930.8 | 3800 | 9070 |
| Left Tibia-Femur Displacement (mm) | 13.4 | 12.6 | 6 | 15 |
| Left Tibia Compression Force Criterion (N) | 3348 | 2877 | 2000 | 8000 |
| Left Upper Tibia Index | 1.24 | 1.64 | 0.4 | 1.3 |
| Left Lower Tibia Index | 0.79 | 0.97 | 0.4 | 1.3 |
| Right Femur Force Criterion (N) | 10048.7 | 10089 | 3800 | 9070 |
| Right Tibia-Femur Displacement (mm) | 13.2 | 12.7 | 6 | 15 |
| Right Tibia Compression Force Criterion | 4010 | 3860 | 2000 | 8000 |
| Right Upper Tibia Index | 0.82 | 1.55 | 0.4 | 1.3 |
| Right Lower Tibia Index | 0.78 | 1.85 | 0.4 | 1.3 |

## DISCUSSION

Test-1 (50% car overlap and 100 km/h closing speed) exhibited an impact energy around 3000 kJ that was higher than reported in previous projects. Such closing speeds can be easily reached in urban or rural road accident scenarios without median barriers. These findings show that head-on collisions with a moving HGV involve high impact energy, presenting significant challenges for vehicle structures and restraint systems [8]. Test-1 also demonstrated that HGV front structures conforming to R93 requirements may still lack sufficient structural strength to protect passenger cars in realistic frontal accident scenarios.

Two research areas have been identified to mitigate this problem: (1) identifying HGV front-end structures that can manage high-energy impacts with cars, and (2) developing restraint systems in cars that reduce occupant injury risk. The SAFE-UP project investigated car-to-HGV frontal crash scenarios and identified three main frontal impact configurations to consider [6]. The work by Mroz et al. [17] highlighted passenger compartment integrity as a prerequisite in a high severity car-to-HGV crash. From a passenger car point of view, a crash configuration of 56/53 km/h, 80% overlap, and 0° impact angle has been suggested for a reference for future legislation and vehicle rating programs. Moderate severity car-to-HGV crashes (39/36 km/h) are adequately represented by the existing 56 km/h full-frontal barrier test for passenger cars. The design of current HGV fronts, including the FUPD, did not provide sufficient compatibility with passenger car fronts and the higher severity (56/53 km/h, -30 $^{O}$ crashes, and the 50% overlap $0^{O}$) crash configurations proved too structurally demanding for the car [17]. Test-1 revealed limitations of the current HGV FUP, initiating the development of an experimental energy-absorbing HGV front. Test-2 resulted in less overall deformation compared to Test-1, but in both cases, the occupant compartment and doors experienced much higher deformation than observed in regulatory or consumer crash programs. This highlights the need for better geometric compatibility for the HGV when addressing high-severity car-to-HGV crashes. The energy-absorbing HGV front-end structure in Test-2 attempted to improve the geometric compatibility between the two vehicles. Previous research efforts, such as VC-COMPAT [12], examined HGV-car geometric compatibility. Still, these studies often assumed a stationary HGV with test speeds ranging from 55-75 km/h and real-world severity levels were not captured.

The modified HGV front in Test-2 generated a smoother crash pulse and achieved a 21% reduction in peak deceleration (58g), while delaying the maximum acceleration from 35 ms to 57 ms compared to Test-1, where the FUP beam failed very early during impact. The backup plate engaged more car structures than Test-1, prevented car underrun, and protected critical HGV components located below the cabin in Test-2. These characteristics indicate the potential for HGVs to play an active role in crash energy management by absorbing impact forces. Extending the crash pulse duration is particularly valuable, as it creates a stable environment for restraint system performance and reduces occupant loading. This benefit can only be realized if the HGV FUP maintains integrity, absorbs part of the collision energy, and prevents entanglement between the car and HGV front. In the later stages of the test, the car's compartment experienced deformation once the energy-absorbing capacity of both vehicles was completely utilized. The experimental honeycomb design was expected to cause the car to glance sideways. However, due to lateral deformation of the honeycomb and a higher relative velocity in the X-direction than predicted by FE simulations (Figure 8**)**, the car absorbed a larger portion of the crash energy than desired. The acceleration pulse in Figure 16 shows that the car's structural members were engaged in the car-to-MPDB assessment, which resulted in greater energy absorption during the first 20 ms. For the same period in both Test-1 and Test-2, the crash pulse dropped to 0 g, indicating that even though Test-2 had a honeycomb front, it was not effectively absorbing energy nor supporting energy absorption processes in the car in early stages of the collision.

Several requirements for HGV front-end structures can be identified: 1) geometrical alignment of front structures must be ensured, 2) energy absorption should be maximised, 3) contact geometries should avoid entanglement facilitating glance off in small overlaps, 3) underride must be prevented, 4) secondary impacts with stiff HGV cabin or chassis components must be avoided, 5) HGV steering mechanisms and sensitive parts must remain protected to maintain post-crash maneuverability. When these conditions are met, occupant protection depends primarily on the restraint systems in both vehicles.

Current safety systems in cars are optimized for car-to-car and car-to-barrier impacts, where crash pulses are shorter and less severe than the long-duration, high-energy pulses observed in car-to-HGV collisions. Additionally, passenger vehicle restraint systems are developed for an intact (non-deformed) occupant compartment. Therefore, maintaining compartment integrity is essential; only then can restraint systems be designed to manage the resulting crash pulse effectively. In both car-to-HGV crash tests conducted, significant compartment deformation made it difficult to draw conclusions on occupant injury values in the passenger car.

Although the front airbag deployed in Test-2, it did not provide complete coverage for the occupant's head, resulting in a high head injury risk. The lower extremities also sustained severe injuries, as existing restraint systems including knee airbags are not specifically tuned for these scenarios. Adaptive restraints systems, airbags covering gaps between the steering wheel and A-pillar, and interior knee padding layouts will help to reduce fatalities in high-severity and high-exposure crashes with restraint systems designed and developed for a wider bandwidth of crash types. Forman et al [18] studied injury criteria target values for high-severity collisions to optimize the existing restraint system using NASS-CDS (2010–2015) and CISS (2017–2019) data across belted occupants in frontal collisions and concluded that injury criteria tailored to crash severity are essential for future restraint system development. A 40% injury risk threshold is feasible and beneficial for high-severity (60 km/h+) crash evaluations.

The findings in this study point two research gaps: (1) there is a need to identify appropriate crash severities and implement stringent regulations or consumer programs to evaluate HGV compatibility, (2) the development of restraint systems specifically tailored to car-to-HGV impact pulses. Addressing these will be essential to achieve safety benefits in this crash configuration involving vehicle fronts.

## CONCLUSION

HGV fronts often lack the structural strength to protect passenger cars in real life frontal accident scenarios as demonstrated in Test-1. Fatal accidents of this type have been reported on Swedish roads with posted speed limits of over 60 km/h, particularly on undivided roads without median barriers [8]. UN R93 does not ensure that HGV fronts provide sufficient lateral load distribution or structural capacity to prevent underride in these partial overlap collisions.

HGVs must be designed with energy absorption capabilities and stable interfaces with their chassis and backup structures that engage a car's energy-absorbing features for various horizontal and vertical overlaps. Otherwise impact loads are directed through the wheels of both vehicles (as a result of underride) and can produce large deformations of the car's A-pillar and do not exploit the existing energy absorbing structures in the passenger car. Moreover, when this proper engagement is achieved, the HGV's own energy-absorption capability will further reduce the pulse severity experienced by the car's occupants.

An experimental HGV front with a honeycomb crash zone supported by a rigid backplate was developed to address the shortcomings identified in previous tests and real-world cases. The new HGV front provided horizontal load spreading for the tested conditions. Still, the high crash severity could not be adequately managed by:

- energy-absorbing mechanisms (honeycomb) when the car remains in contact with the HGV front and experiences large longitudinal velocity changes or
- passenger car glance off to reduce long duration loading of passenger car structures, demonstrated in the FE study.

Future HGV front safety systems should be designed so FUP systems remain structurally intact and provide geometrical compatibility with the passenger car's energy absorbing structures, while preventing the vehicle from becoming caught or entangled with the HGV's structure. Energy absorption of all vehicle structures involved (car and HGV) must be maximized while preventing the underrun of the HGV and protecting the HGV's steering and braking systems. In cases of smaller overlaps, these systems could promote a glance-off motion during frontal collisions with passenger cars. This glance-off approach can reduce intrusions into the car's occupant compartment, support the effectiveness of restraint systems, and lower the risk of severe injury of all vehicle occupants involved.

## REFERENCES


[1] "Vehicle mileage for Swedish-Registered Vehicles, Vehicles kilometres 2024 ", 2025. [Online]. Available: https://www.trafa.se/en/road-traffic/driving-distances-with-swedish-registered-vehicles/

[2] P. Hurtig *et al.*, "Analysis of road safety trends 2022 : Management by objectives for road safety work towards the 2030 interim targets," in "Trafikverkets publikationer," Trafikverket, Borlänge, 978-91-8045-196-3 (ISBN), 2023 2023. [Online]. Available: http://urn.kb.se/resolve?urn=urn:nbn:se:trafikverket:diva-12242

[3] "Unique Swedish work with new truck front to save more motorists' lives." https://bransch.trafikverket.se/en/startpage/operations/Operations-road/vision-zero-academy/Vision-Zero-and-ways-to-work/euro-ncap/unique-swedish-work-with-new-truck-front-to-save-more-motorists-lives/.

[4] M. S. Hatun Atasayar, Martin Donabauer (KFV), "European Commission (2025) Annual statistical report on road safety in the EU, 2025. European Road Safety Observatory.," Directorate General for Transport, Brussels, European Commission, February 2025. [Online]. Available: https://road-safety.transport.ec.europa.eu/european-road-safety-observatory/statistics-and-analysis-archive/annual-accident-report_en

[5] "Fatality Facts 2023- Large trucks " Insurance Institute for Highway Safety (IIHS), Highway Loss Data Institute (HLDI). https://www.iihs.org/research-areas/large-trucks.

[6] V. L. A. Balint, C. Vogl, J. Stoll, L. Schories, L. Annan, G. Baroda Sudhakaran, P. Huertas Leyva, T. Pallacci, M. Östling, D. Schmidt and R. Schindler, "D2.6 Use Case Definitions and Initial Safety-Critical Scenarios," Horizon 2020 Project proactive SAFEty systems and tools for a constantly UPgrading road environment (SAFE-UP)," 2021.

[7] R. Schindler, M. Jänsch, and N. Parera, "D5.1: Safety issues for safety system design, AEROFLEX," 2018.

[8] R. Fredriksson, R. Thomson, K. Mroz, D. Kruse, and F. Törnvall, "Frontal Crash Incompatibility of Heavy Goods Vehicle in Crash Test With Passenger Car," presented at the Enhanced Safety of Vehicles International Technical Conference, Yokohama, Japan, 2023.

[9] P. H. Rikard Fredriksson, Peter Larsson, Magnus Lindholm, Kenneth Svensson (Trafikverket), Khabat Amin, Staffan Berge Holmbom, Ole Brus (Transportstyrelsen), "Analys av trafiksäkerhetsutvecklingen 2024," 2025.

[10] "UNECE, Regulation R93: Front Underrun Protective Devices," 1994.

[11] A. Krusper and R. Thomson, "Truck frontal underride protection - Compatibility factors influencing passenger car safety," *International Journal of Crashworthiness,* vol. 17, pp. 217-232, 04/01 2012, doi: 10.1080/13588265.2011.648514.

[12] M J Edwards (TRL) *et al.*, "Improvement of Vehicle Crash Compatibility through the Development of Crash Test Procedures (VC-COMPAT) " TRL and TNO, 2007.

[13] "European Commission, JRC Publications Repository." https://publications.jrc.ec.europa.eu/repository/handle/JRC139954.

[14] IIHS. "Test protocols and technical information IIHS 2.0 side impact." https://www.iihs.org/ratings/about-our-tests/test-protocols-and-technical-information.

[15] Mervyn Edwards, Richard Cuerden, and H. D. T. Limited, "Current Status of the Full Width Deformable Barrier Test," presented at the 20th International Technical Conference on the Enhanced Safety of Vehicles (ESV), 2007. [Online]. Available: http://www-nrd.nhtsa.dot.gov/departments/esv/20th/.

[16] "Mobile Progressive Deformable Barrier." https://www.euroncap.com/en/car-safety/the-ratings-explained/adult-occupant-protection/frontal-impact/mobile-progressive-deformable-barrier/ (accessed.

[17] K. Mroz, M. Östling, and N. Lubbe, "Passenger cars in head-on crashes with heavy goods vehicles: For what severity should future car restraint systems be designed?," 2023.

[18] J. Forman, M. Östling, K. Mroz, and N. Lubbe, "Potential Injury Criteria for Collisions with Heavy Goods Vehicles," 2023.

## APPENDIX A

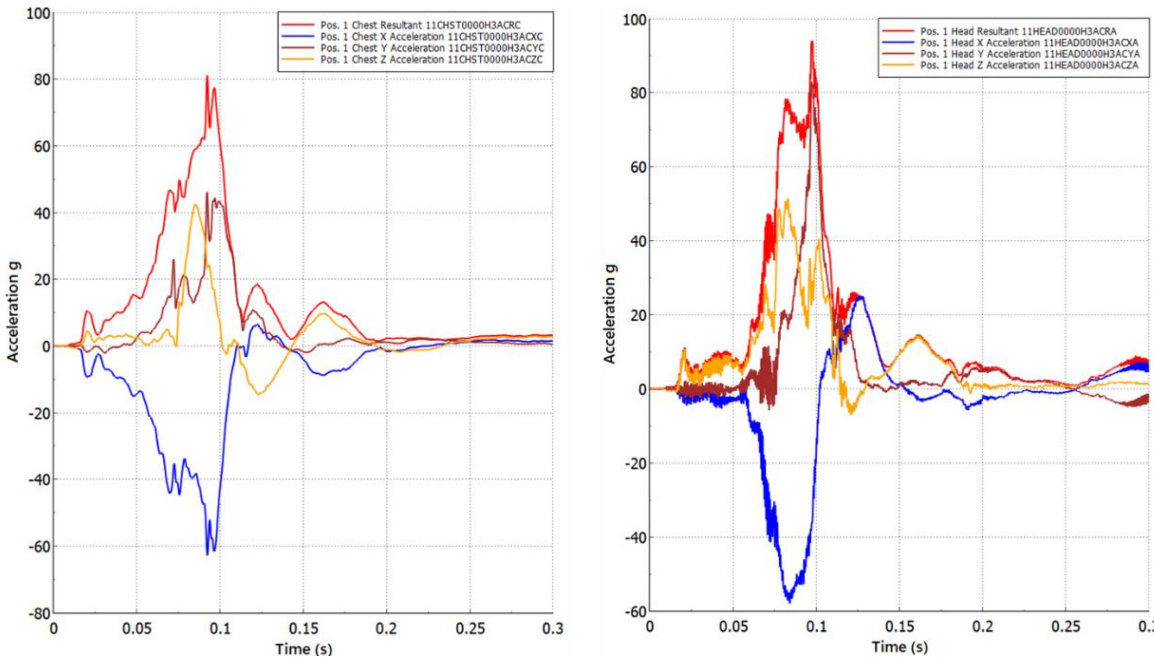


***Figure A1: HIII 50th percentile driver dummy chest accelerations (left) and head accelerations (right)***